

**B. TECH. PROJECT  
REPORT**

**On**

**Effect of Electrode Shape  
on TIG Arc Behavior**

**BY**

**Mohit Singhal (180003033)**

**Prachi Kuril (180003040)**



**DEPARTMENT OF MECHANICAL ENGINEERING  
INDIAN INSTITUTE OF TECHNOLOGY INDORE**

**May 2022**



# Effect of Electrode Shape on TIG Arc Behavior

**A PROJECT REPORT**

*Submitted in partial fulfillment of the  
requirements for the award of the degrees*

*of*

**BACHELOR OF TECHNOLOGY**

**in**

**MECHANICAL ENGINEERING**

*Submitted by:*

**Mohit Singhal (180003033)**

**Prachi Kuril (180003040)**

*Guided by:*

**Dr. Yuvraj Kumar Madhukar (Assistant Professor, IIT Indore )**



**INDIAN INSTITUTE OF TECHNOLOGY INDORE**

**May 2022**



## CANDIDATE’S DECLARATION

We hereby declare that the project entitled “**Effect of electrode shape TIG arc behavior**” submitted in partial fulfillment for the award of the degree of Bachelor of Technology in ‘Mechanical Engineering’ completed under the supervision of **Yuvraj K. Madhukar (Assistant Professor, IIT Indore)**, IIT Indore is an authentic work.

Further, I/we declare that I/we have not submitted this work for the award of any other degree elsewhere.



**Mohit Singhal**



**Prachi Kuril**

---

## CERTIFICATE by BTP Guide(s)

It is certified that the above statement made by the students is correct to the best of my/our knowledge.



24/05/22

**Dr. Yuvraj Kumar Madhukar**

Assistant Professor

Department of Mechanical Engineering

IIT Indore



## Preface

This report on “**Effect of electrode shape TIG arc behavior**” is prepared under the guidance of Dr. Yuvraj K. Madhukar (Assistant Professor, IIT Indore).

Through this report, we have tried to understand the influence of different parameters like the current and shape of the electrode on the TIG welding arc with simulation in COMSOL. We have tried to the best of our abilities and knowledge to explain the content in a lucid manner.



**Mohit Singhal**



**Prachi Kuril**

B.Tech. IV Year

Department of Mechanical Engineering

IIT Indore



## Acknowledgments

We wish to thank **Dr. Yuvraj K. Madhukar** for allowing us to work on this project. We are grateful for his guidance and cooperation throughout the project. We are indebted to him for sharing his valuable knowledge and expertise in the field of Additive Manufacturing.

Our sincere thank goes to **Mr. Anas Khan** for his help and support

We are grateful for the love and support are given to us by our family and friends during this time. We would also like to express our gratitude towards anyone who might not be named here but has extended their support to us in this process.



**Mohit Singhal**



**Prachi Kuril**

B.Tech. IV Year

Department of Mechanical Engineering

IIT Indore



## **Abstract**

Tungsten inert gas (TIG) welding has been extensively utilized for wire arc additive manufacturing (WAAM) applications. The presented work investigates the formed arc characteristics for different electrode geometry to enhance the overall process efficiency. The electrode sharpening angle was varied at 30°, 60°, 90°, and 107°. COMSOL plasma module has been utilized for the computation of temperature field, arc pressure, heat flux, and current density variation in arc column. The simulated model was then used to study the influence of input current from 100A to 200A. It was observed that an increase in electrode sharpen angle increases the arc concentration to a narrow area, whereas the increase in arc input current widens the concentration zone at the anode. An experimental study performed at different currents and recorded high-speed arc imaging also confirms the same. It typically follows the gaussian distribution. However, the magnitude of the temperature field, arc pressure, heat flux, and current density varies in arc columns. The volumetric distribution of these properties was higher near the cathode or electrode for a higher electrode angle and was found to be a good choice for WAAM.



# Table of Contents

Candidate's Declaration	i
Certificate By Btp Guide(S)	i
Preface	ii
Acknowledgments	iii
<b>Abstract</b>	<b>10</b>
<b>Table of Contents</b>	<b>12</b>
<b>List of Figures</b>	<b>14</b>
<b>List of Tables</b>	<b>16</b>
<b>Table of abbreviation and Symbols</b>	<b>18</b>
<b>Chapter1: Introduction</b>	<b>20</b>
<b>Chapter 2: Methodology</b>	<b>24</b>
2.1 Mathematical Model Definition:	24
2.1.1 Equations:	25
2.1.2 Model Diagram:	27
2.2.3 Boundary Conditions:	28
2.2 Simulation Model Definition:	29
2.2.1 Parameters	29
2.2.2 Geometry	30
2.2.3 Materials	30
2.2.4 Electric Currents	31
2.2.5. Magnetic Fields	32
2.2.6. Heat Transfer In Fluids	32
2.2.7. Laminar Flow	33
2.3 Observation From Simulation:	34
2.3.1 30° Electrode Sharpening Angle	34

2.3.2 60° Electrode Sharpening Angle	38
2.3.3 90° Electrode Sharpening Angle	42
2.3.4 107° Electrode Sharpening Angle	46
2.4 Experiment:	50
2.4.1 Experimental Setup	50
2.4.2 Mach3 CNC Software	51
2.4.3 Observations	51
<b>Chapter3: Results and Discussion</b>	<b>54</b>
<b>Chapter4: Conclusion and Future Scope</b>	<b>58</b>
4.1 Conclusion	58
4.2 Future Scope:	58
<b>References</b>	<b>60</b>

## List of Figures

1. TIG welding principle
2. Feeding of filler material
3. Computational domain
4. The geometry of model
5. Materials
6. Electrode sharpening angle
7. Temperature profile at 100A at 30 degrees
8. Temperature profile at 150 A at 30 degrees
9. Temperature profile at 200A at 30 degrees
- 10.Radial evolution of Temperature at the center at 30 degrees
- 11.Radial evolution of Pressure at the center at 30 degrees
- 12.Radial evolution of Heat Flux at the center at 30 degrees
- 13.Radial evolution of Current density at the center at 30 degrees
- 14.Temperature profile at 100A at 60 degrees
- 15.Temperature profile at 150 A at 60 degrees
- 16.Temperature profile at 200A at 60 degrees
- 17.Radial evolution of Temperature at the center at 60 degrees
- 18.Radial evolution of Pressure at the center at 60 degrees
- 19.Radial evolution of Heat Flux at the center at 60 degrees
- 20.Radial evolution of Current density at the center at 60 degrees
- 21.Temperature profile at 100A at 90 degrees
- 22.Temperature profile at 150 A at 90 degrees
- 23.Temperature profile at 200A at 90 degrees

- 24.Radial evolution of Temperature at the center at 90 degrees
- 25.Radial evolution of Pressure at the center at 90 degrees
- 26.Radial evolution of Heat Flux at the center at 90 degrees
- 27.Radial evolution of Current density at the center at 90 degrees
- 28.Temperature profile at 100A at 107degrees
- 29.Temperature profile at 150 A at 107 degrees
- 30.Temperature profile at 200A at 107 degrees
- 31.Radial evolution of Temperature at the center at 107 degrees
- 32.Radial evolution of Pressure at the center at 107 degrees
- 33.Radial evolution of Heat Flux at the center at 107 degrees
- 34.Radial evolution of Current density at the center at 107 degrees
- 35.Experiment setup
- 36.Mach3 control board
- 37.Mach3 control software
- 38.Arc image at 100A at 90 degrees
- 39.Arc image at 150A at 90 degrees
- 40.Arc image at 200A at 90 degrees
- 41.Arc image at 100A at 67degrees
- 42.Arc image at 150A at 67 degrees
- 43.Arc image at 200A at 67 degrees
- 44.Arc image at 100A at 50 degrees
- 45.Arc image at 150A at 50 degrees
- 46.Arc image at 200A at 50 degrees
- 47.Temperature profiles at 100,150,200A respectively at 60-degree angle
48. Arc images at 100,150,200A respectively at a 67-degree angle
49. The heat flux variation at 150 A at different sharpening angles

## List of Tables

1. Abbreviations and symbols
2. Boundary Conditions
3. Parameters of Model
4. Materials
5. Condition for electric currentsCondition for Heat Transfer
6. Condition for laminar flow
7. Parameters at 30 degrees
8. Parameters at 60 degrees
9. Parameters at 90 degrees
10. Parameters at 107 degrees



## Table of abbreviation and Symbols

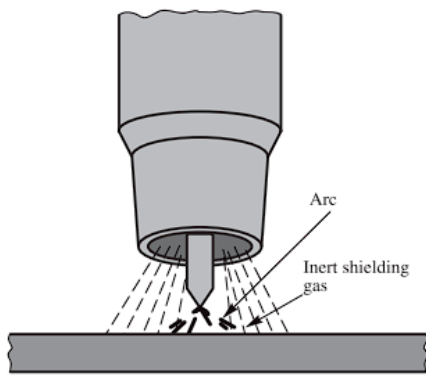
$v$	velocity (m/s)
$\rho$	density (kg/m <sup>3</sup> )
$p$	pressure
$j$	current density (A/m <sup>3</sup> )
$B$	magnetic flux density (Wb/m <sup>2</sup> )
$V$	electric potential
$g$	gravity
$w$	vorticity
$T$	temperature (K)
$k$	thermal conductivity (W/m.k)
$A$	magnetic potential vector
$\beta$	metal thermal expansion
$\sigma_b$	Stefan- Boltzmann constant
$T_{ef}$	solidus temperature
$\phi_z$	anode work function
$\sigma$	electrical conductivity (1/ohm. m)

**Table 1: Abbreviations and symbols**



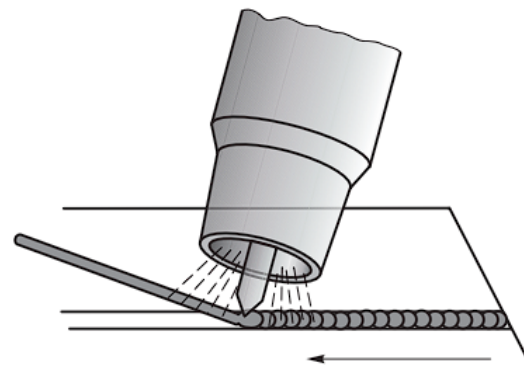
# Chapter1: Introduction

Tungsten Inert Gas Welding (TIG), also known as GAS Tungsten Arc Welding (GTAW), is an electric arc welding process that creates fusion energy between the workpiece and the tungsten electrode using an electric arc. An inert shielding gas shields the electrode, the arc, and the weld pool from the damaging effects of the ambient air during the welding process. A gas nozzle directs the shielding gas to the welding zone, where it replaces atmospheric air. Argon is the most widely utilized shielding gas due to its inexpensive cost. TIG welding differs from MIG/MAG and MMA welding in that the electrode is not consumed.



*TIG welding Principle*

**figure 1**



*Feeding of filler material*

**figure 2**

The numerical simulation's complexity stems from the close relationship between numerous phenomena engaged in the process. Over a wide temperature range of 300 K to over 20,000 K, the heating Joule effect creates a thermal plasma comprising electrons, ions, and neutral species. The workpiece is then heated on the upper surface by arc-plasma conduction and electron flow.

Because of its many advantages, the TIG welding technique has a wide range of applications. It provides good protection of the weld pool by an inert shielding gas, no need for post-weld treatment because no slag or spatter is created, and concentrated heating of the workpiece, among others. TIG welding is commonly used in industries that require high-quality welding, such as the chemical industry, nuclear industry, petrochemical industry, offshore industry, combined heat and power plants, food industry, and so on.

Many numerical models have been developed for GTAW But most of them take only one part of the welding process either anode, cathode, or plasma arc resulting in some boundary conditions which don't mimic the real situation. The right way to understand this arc behavior is to consider all three model parts. Taking this into consideration, a mathematical model is developed in [1].

In the present work, the model ( present in [1], which is taking all three parts cathode, anode, and plasma into consideration ) is simulated in COMSOL, then used to study the influence of current and shape of the electrode's tip on heat flux, temperature and pressure. We have taken three current values 100A, 150A, and 200A for each electrode. Simulation has been done on four king Tungsten Electrode tip shapes.

This thesis is organized as follows: Chapter 2. describes the methodology taken to approach the objectives. Sections 2.1 and 2.2 detail the model's mathematical and simulated definition respectively. Section 2.3 deals with the observation that we got from the simulation of the model and shows the variation of temperature, heat-flux, current density, and pressure with respect to different electrode sharpening angles and input current. Section 2.4 deals with the experimental observations that we have captured while conducting the experiment. It displays some images of TIG arc with different electrode sharpening angles and input currents. Chapter 3. discusses the observation and tries to extract some interesting results from work done. Chapter 4. concludes the work done in this project and discusses the scope for work to be done in the future.



## Chapter 2: Methodology

### 2.1 Mathematical Model Definition:

Mathematical modeling is the process of attempting to mathematically define a nonmathematical situation, phenomenon, and its interactions, as well as discovering mathematical patterns within these situations and phenomena. The widest and most liberal definition of mathematical modeling is this one. It includes the steps of discovering relationships, doing mathematical analyses, obtaining results, and reinterpreting the model. For GTAW, many numerical models have been constructed. However, most of them only use one portion of the welding process, such as anode, cathode, or plasma arc, resulting in boundary conditions that aren't realistic. Considering all three model pieces is the best method to comprehend this arc behavior. Taking this into consideration, a mathematical model is developed in [1].

For the mathematical formulation of the multiphysics issue, the following assumptions are taken into account::

1. The research is limited to spot GTAW and uses an axisymmetric coordinate system.
2. Metal vapors have no effect on plasma characteristics since the arc column is believed to be at Local Thermodynamic Equilibrium (LTE)..
3. Molten metal and gas plasma are both incompressible..

### 2.1.1 Equations:

In the plasma and anode domains, the velocity and pressure fields are estimated, and the temperature field is determined in the three zones using the conservation equations, as follows:

(1) Conservation of mass

$$\nabla \cdot \vec{v} = 0$$

(2) Conservation of momentum

$$\rho \left( \frac{\partial \vec{v}}{\partial t} + \vec{v} \cdot \nabla \vec{v} \right) = -\nabla p + \nabla \cdot \left[ \mu (\nabla \vec{v} + {}^t \nabla \vec{v}) \right] \\ + \vec{j} \times \vec{B} + \rho_0 \vec{g} (1 - w_p \beta (T - T_{ref}))$$

(3) Conservation of energy

$$\rho c_p^{eq} \left( \frac{\partial T}{\partial t} + \vec{v} \cdot \nabla T \right) = \nabla \cdot (k \nabla T) + S_v$$

In the anode and cathode regions, the volumetric heat source is the Joule effect

$$S_v = \vec{j} \cdot \vec{E}$$

whereas in the arc plasma region the enthalpies flux and radiation losses are added

$$S_v = \vec{j} \cdot \vec{E} + \frac{5k_B}{2e} \vec{j} \cdot \nabla T - 4\pi\epsilon_N$$

Calculating the current density  $j$  and the magnetic flux  $B$  is required to determine the electromagnetic forces and the Joule effect in both the arc plasma and the workpiece.

As a function of the electric potential  $V$  and the magnetic potential vector  $A$ , the linked current continuity and magnetic potential equations are determined as follows:

$$\begin{aligned}\nabla \cdot (\sigma \nabla V) &= 0 \\ \nabla \times \left( \frac{1}{\mu_0} \nabla \times \vec{A} \right) + \sigma \nabla V &= \vec{0}\end{aligned}$$

The current density, electric field, and magnetic flux are then calculated from  $V$  and  $A$  as follows:

$$\vec{E} = -\nabla V; \quad \vec{j} = -\sigma \nabla V; \quad \vec{B} = \nabla \times \vec{A}$$

### 2.1.2 Model Diagram:

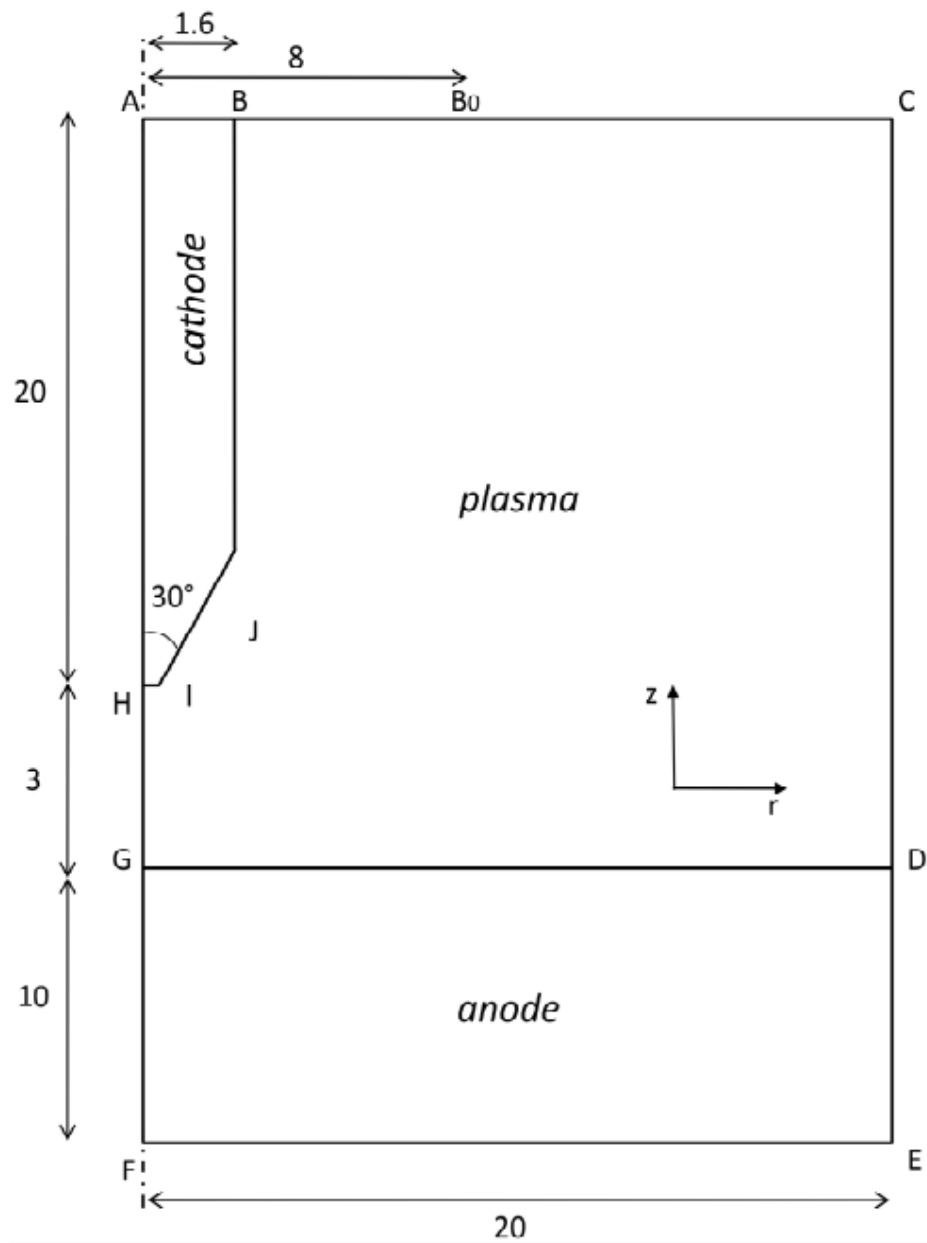


figure 3: Computational domain (dimensions in mm)

### 2.2.3 Boundary Conditions:

<b>AB</b>	$T = T_0; \quad \vec{j} \cdot \vec{n} = \frac{I}{\pi R_c^2}$
<b>BB0</b>	$T = T_0; \quad \vec{v} \cdot \vec{n} = -U_{gaz}; \quad \vec{j} \cdot \vec{n} = 0; \quad \vec{A} \times \vec{n} = 0$
<b>B0C</b> <b>CD</b>	$T = T_0; \quad \vec{j} \cdot \vec{n} = 0; \quad p = p_0;$ $\vec{n} \cdot \underline{\underline{\tau}} \cdot \vec{n} = 0; \quad \vec{A} \times \vec{n} = \vec{0}$
<b>DE</b> <b>EF</b>	$\vec{q} \cdot \vec{n} = h_c(T - T_0); \quad \vec{v} = \vec{0}; \quad V = 0; \quad \vec{A} \times \vec{n} = 0$
<b>FA</b>	$\vec{q} \cdot \vec{n} = 0; \quad \vec{v} \cdot \vec{n} = 0; \quad \vec{j} \cdot \vec{n} = 0; \quad \vec{B} = \vec{0}$
<b>GD</b>	$[-k\nabla T \cdot (-\vec{n})]_{anode} = [-k\nabla T \cdot (-\vec{n})]_{plasma} +  \vec{j} \cdot \vec{n}  \phi_a - \epsilon \sigma_B T^4$ $\mu \frac{\partial(\vec{v} \cdot \vec{s})}{\partial \vec{n}} = \vec{\tau}_a + f_L \frac{\partial \gamma}{\partial T} \frac{\partial T}{\partial \vec{s}}$ $\vec{v} \cdot \vec{n} = 0; \quad \llbracket \vec{j} \cdot \vec{n} \rrbracket = 0$
<b>HB</b>	$[-k\nabla T \cdot (-\vec{n})]_{cathode} = [-k\nabla T \cdot (-\vec{n})]_{plasma} + j_i V_i - j_e \phi_c - \epsilon \sigma_B T^4$ $\vec{v} = \vec{0}; \quad \llbracket \vec{j} \cdot \vec{n} \rrbracket = 0$

Table 2: Boundary Conditions

## 2.2 Simulation Model Definition:

This model is based on work presented in Ref. 1. In Ref. 1 The authors develop a complex model that includes the description of the weld pool under the action of a pulsed arc. This work only simulates the plasma and the transfer of heat and currents in the metals neglecting the weld pool, and a DC excitation is used. These simplifications allow a model that solves fast and can be used to understand fundamental physical effects and to use as initial conditions for a time-dependent model.

The model is solved using a stationary study. Multiple values of current are set at the cathode and the bottom plate is grounded for different cases. In the gap between the electrodes, an argon plasma arc is created that heats the metal electrodes and surrounding gas. A shielding flow is added along with the cathode.

**Software Used:** COMSOL MULTIPHYSICS, version- 6.0

### 2.2.1 Parameters

Name	Expression	Description
I0	100[A] / 150[A] / 200[A]	Current
J0	$-I0/(\pi*(1.6[\text{mm}]^2)$	Normal Current density
U0	3[m/s]	Inlet velocity

**Table 3: Parameters of Model**

## 2.2.2 Geometry

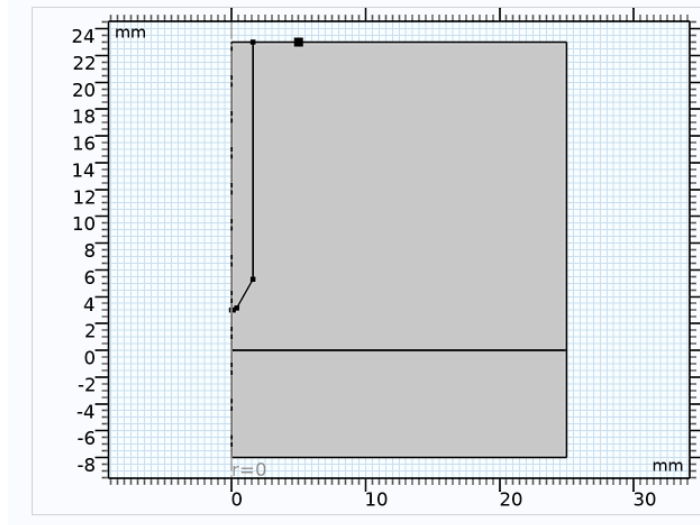


figure 4:the Geometry

Note: In this geometry, only the shape of the electrode tip is modified for different cases, the rest is the same for all cases.

## 2.2.3 Materials

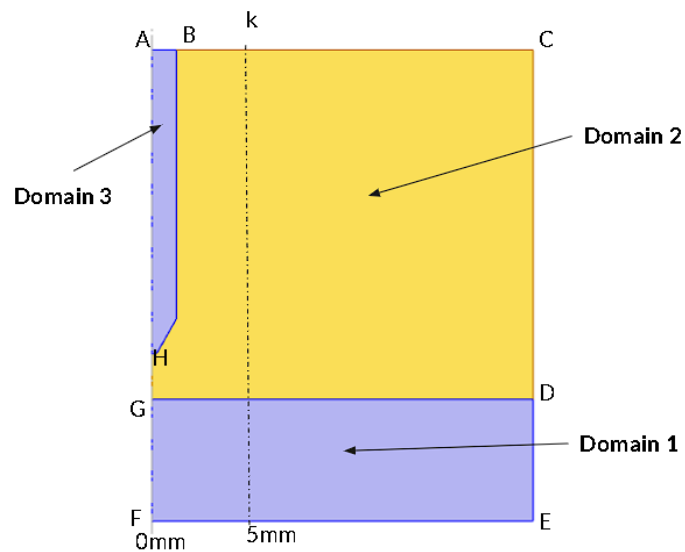


figure 5: Materials

<b>Material</b>	<b>Area</b>
Argon (mat1)	Domain 2
Steel AISI 4340 (mat2)	Domain 1
Tungsten (mat3)	Domain 3

**Table 4: Materials**

## 2.2.4 Electric Currents

### Equations

$$\nabla \cdot \mathbf{J} = Q_{j,v}$$

$$\mathbf{J} = \sigma \mathbf{E} + \mathbf{J}_e$$

$$\mathbf{E} = -\nabla V$$

### Conditions

FE, DE	Ground	$V=0$
AB	Normal Current Density	$J_n = J_0$

**Table 5: Condition for electric currents**

## 2.2.5. Magnetic Fields

### Equations

$$\nabla \times \mathbf{H} = \mathbf{J}$$

$$\mathbf{B} = \nabla \times \mathbf{A}$$

$$\mathbf{J} = \sigma \mathbf{E} + \sigma \mathbf{v} \times \mathbf{B} + \mathbf{J}_e$$

## 2.2.6. Heat Transfer In Fluids

### Equations

$$\rho C_p \mathbf{u} \cdot \nabla T + \nabla \cdot \mathbf{q} = Q + Q_p + Q_{vd}$$

$$\mathbf{q} = -k \nabla T$$

### Conditions

Domain 1,2,3	Initial Value	$T = 300\text{K}$
Domain 1,2	Volume Reference Temp	$T_{\text{ref}} = 300\text{K}$
AB, BC,CD	Boundary	$T_0 = 300\text{K}$
DE,EF	Heat Flux	$h=200 \text{ W}/(\text{m}^2.\text{K})$
GD, HB	Boundary Heat Source	$Q_b=-0.4*\sigma_{\text{const}}*T^4$

**Table 6: Condition for heat transfer**

## 2.2.7. Laminar Flow

### Equations

$$\rho(\mathbf{u} \cdot \nabla)\mathbf{u} = \nabla \cdot [-p\mathbf{I} + \mathbf{K}] + \mathbf{F}$$

$$\nabla \cdot (\rho\mathbf{u}) = 0$$

### Conditions

---

BK	Inlet Velocity	U=U0
----	----------------	------

---

**Table 7: Condition for laminar flow**

## 2.3 Observation From Simulation:

This work investigates the formed TIG arc characteristics for different electrode geometry to enhance the overall process efficiency. The electrode sharpening angle was varied at  $30^\circ$ ,  $60^\circ$ ,  $90^\circ$ , and  $107^\circ$ . COMSOL plasma module has been utilized for the computation of temperature field, arc pressure, heat flux, and current density variation in arc column. The influence of input current from 100A to 200A was then investigated using the simulated model.

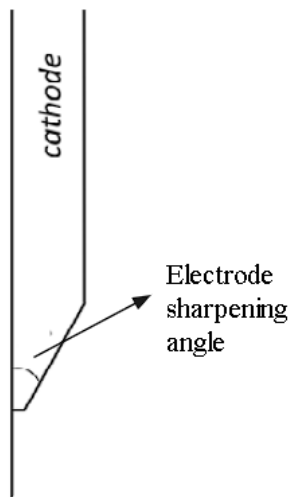


*figure 6*

### 2.3.1 $30^\circ$ Electrode Sharpening Angle

Here we are going to see variations in temperature, current density, pressure, and heat flux at 100A, 150A, and 200A for the electrode sharpening angle of 30 degrees.

Figs 7, 8, and 9 show the temperature profile for different input currents 100A,150A, and 200A respectively for the electrode sharpening angle of 30°. From these figures, it is observed that increasing the input current widens the concentration zone of temperature at the anode.

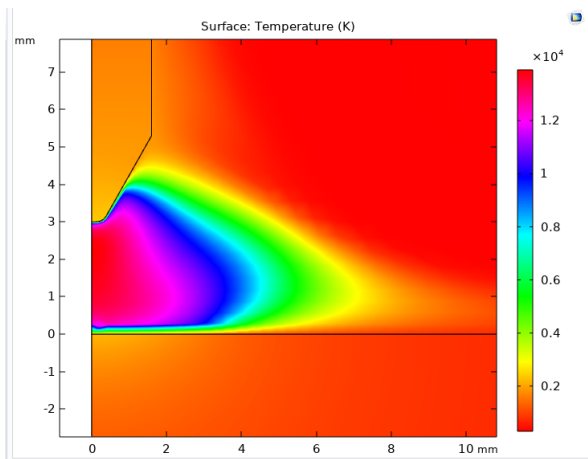


**Fig 7: Temperature Profile at 100A**

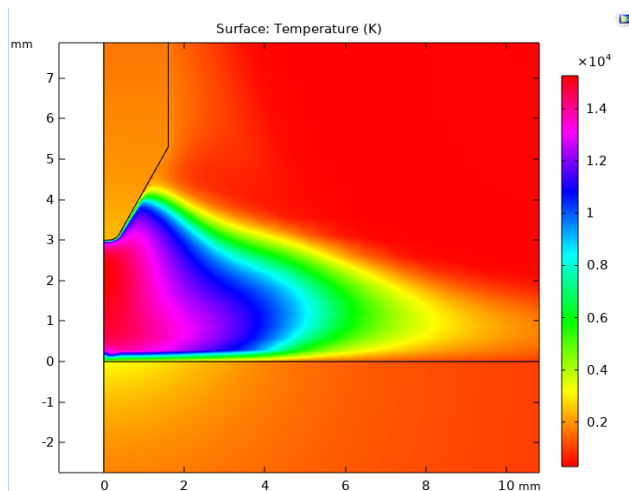


**Fig 8: Temperature Profile at 150A**

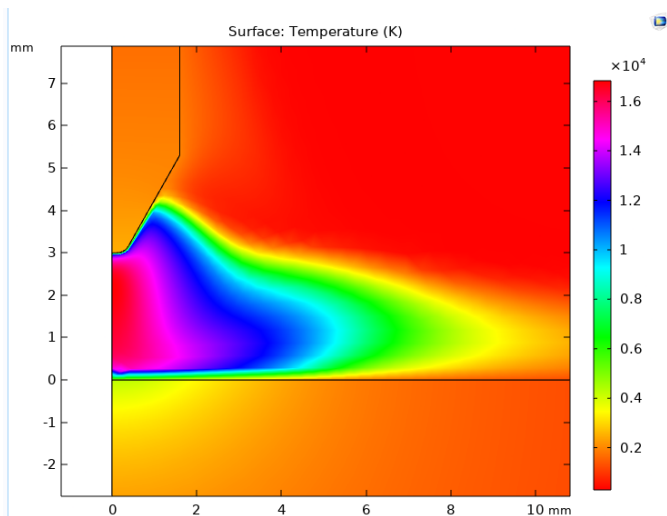


**Fig 9: Temperature Profile at 200A**

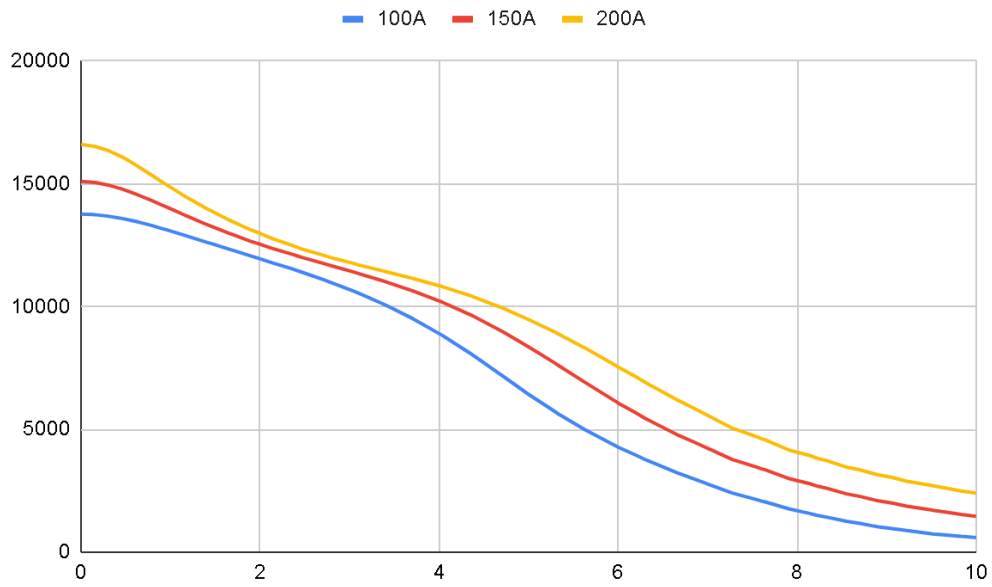


**Figure 10: Radial evolution of Temperature at the center of the anode and cathode**

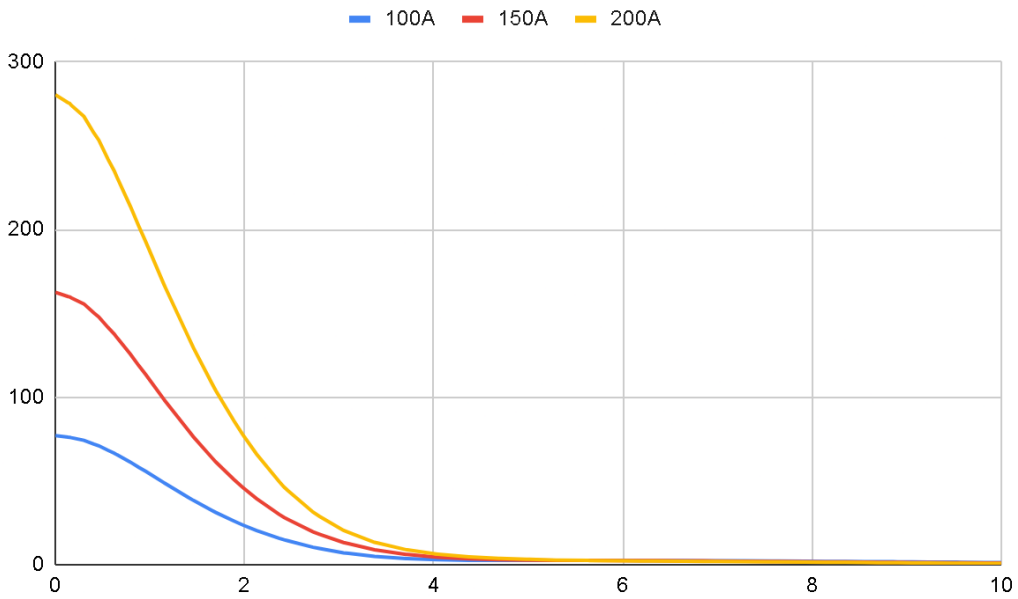


**Figure 11: Radial evolution of Pressure at the center of the anode and cathode**

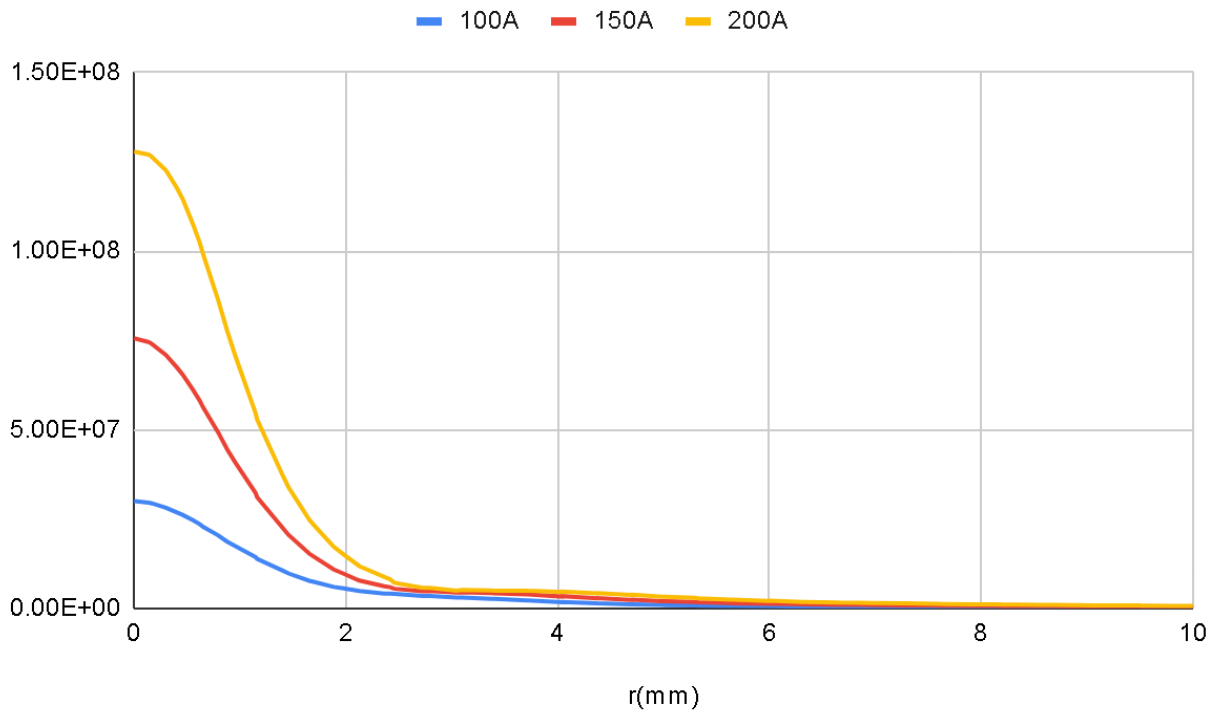


Figure 12: Radial evolution of HeatFlux magnitude at the center of the anode and cathode

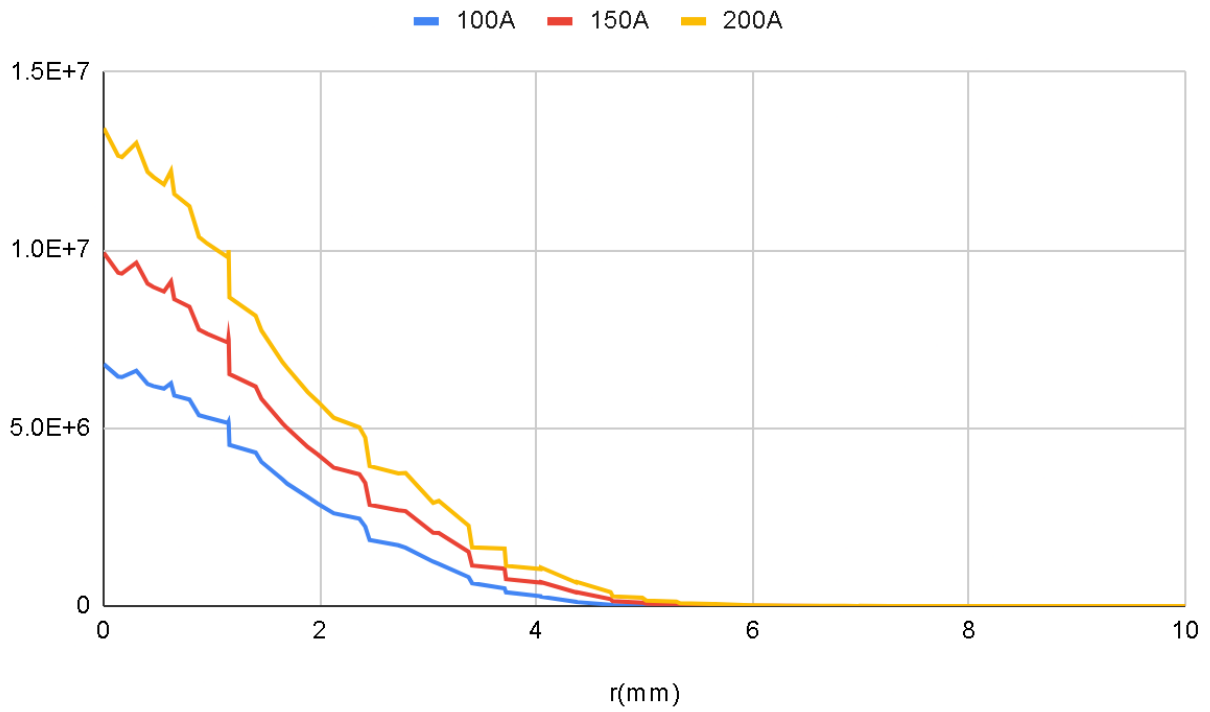


Figure 13: Radial evolution of Current Density at the center of anode and cathode

The radial evolution of temperature, pressure, heat flux, and current density at the center of cathode and anode for the different input currents are shown in Fig 10,11,12, and 13 respectively. An increment in the input current increases all these properties at every point. From the figure, it can be seen that all of these properties are typically following gaussian distribution.

<b>Input Current</b>	100A	150A	200A
<b>Max Temperature</b>	13917 K	15260 K	16834 K
<b>Max Pressure</b>	138 Pa	335 Pa	619 Pa
<b>Max HeatFlux</b>	1.46E+08 W/m <sup>2</sup>	2.23E+08 W/m <sup>2</sup>	2.98E+08 W/m <sup>2</sup>
<b>Max Current Density</b>	1.51E+08 A/m <sup>2</sup>	1.93 E+08 A/m <sup>2</sup>	2.34E+08 A/m <sup>2</sup>

**Table 8: Parameters at 30 degrees**

### **2.3.2 60° Electrode Sharpening Angle**

Figs 14, 15 and 16 show the temperature profile for different input currents 100A, 150A, 200A respectively for the electrode sharpening angle of 60°. From these figures, it is again observed that increasing the input current widens the concentration zone of temperature at the anode.

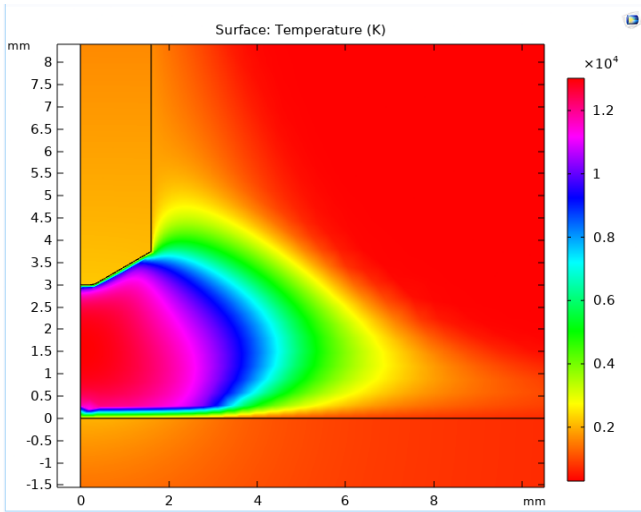


**Fig 14: Temperature Profile at 100A**

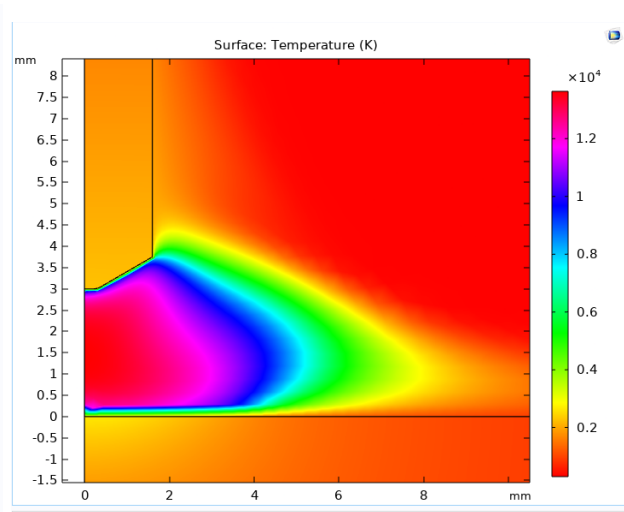


**Fig 15: Temperature Profile at 150A**

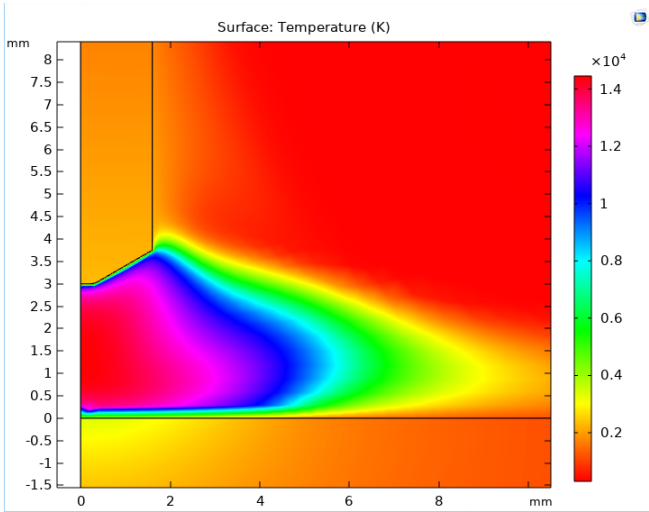


**Fig 16: Temperature Profile at 200A**

The radial evolution of temperature, pressure, heat flux, and current density at the center of the cathode and anode for the different input currents are shown in Fig 17,18,19, and 20 respectively. An increment in the input current increases all these properties at every point. From the figure, it can be seen that all of these properties are typically following gaussian distribution.

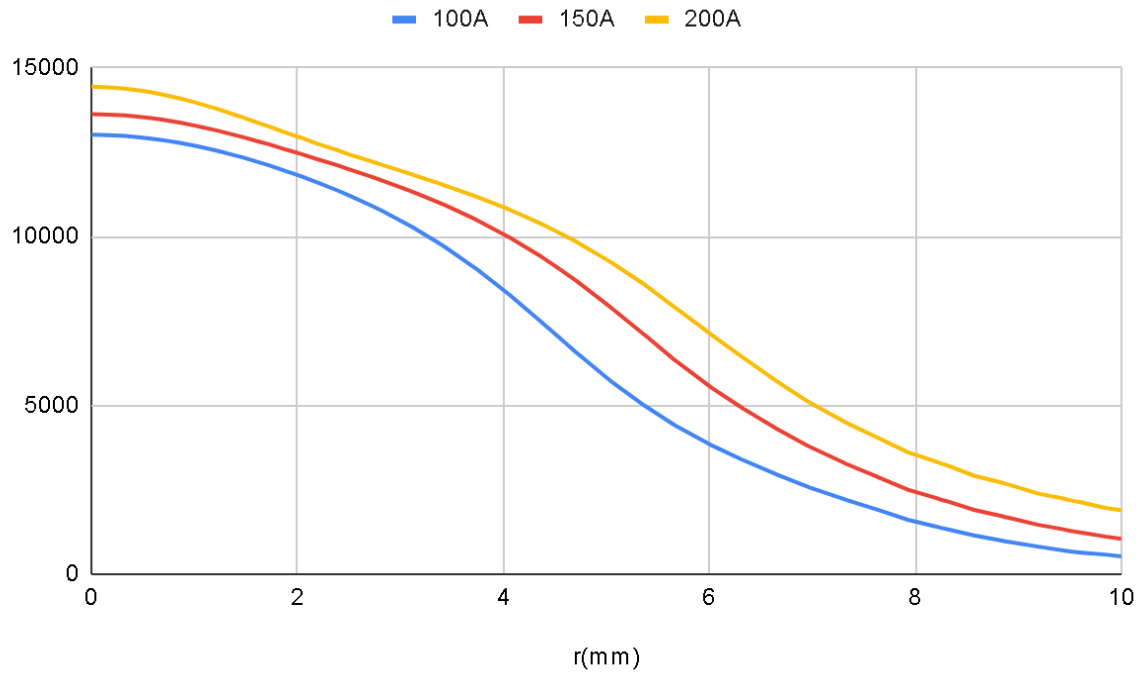


**Figure 17:: Radial evolution of Temperature at the center of the anode and cathode**

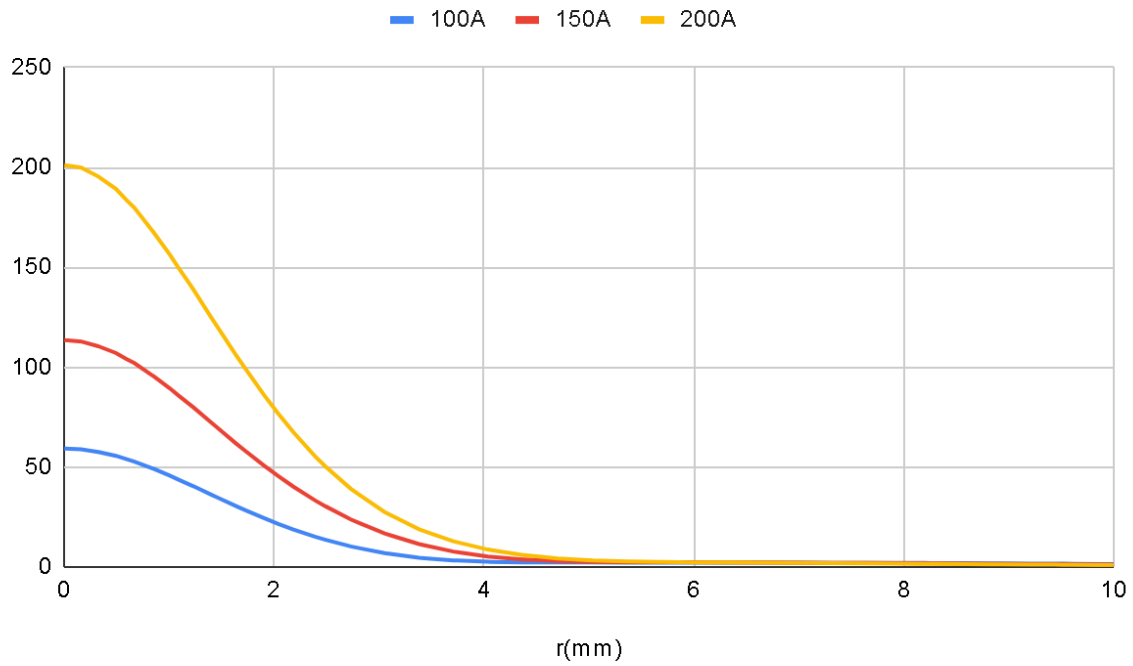


**Figure 18: Radial evolution of Pressure at the center of the anode and cathode**

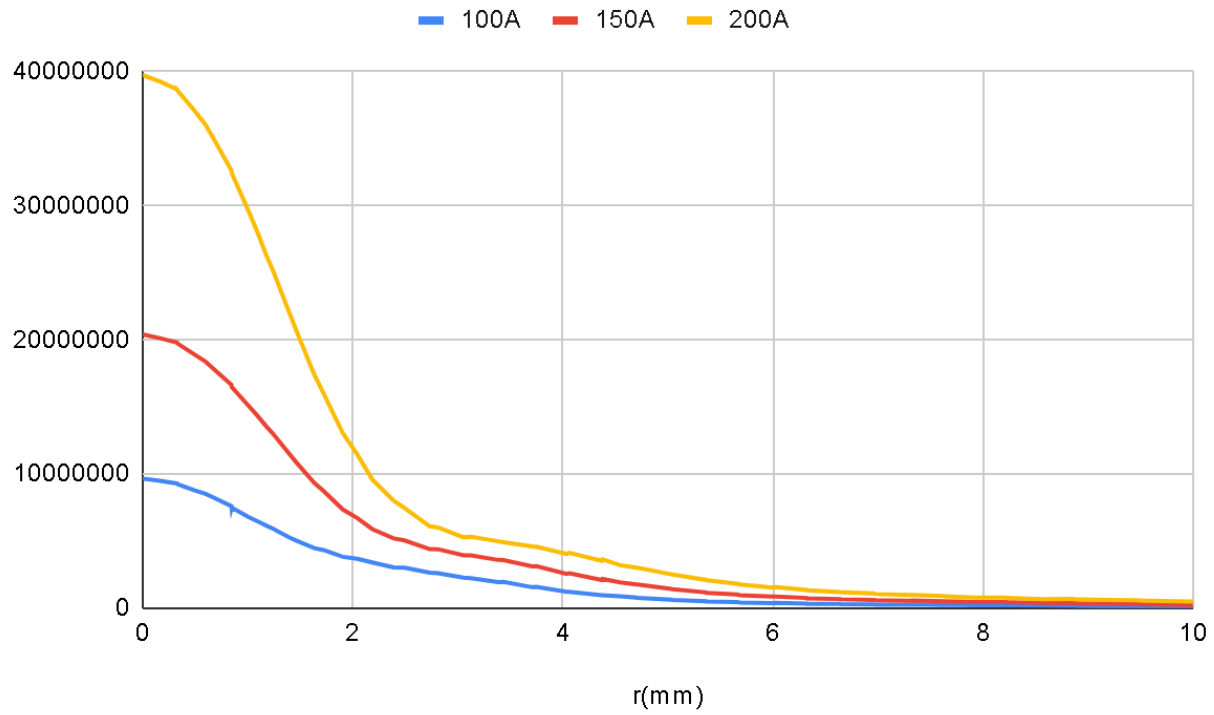


Figure 19: Radial evolution of heat flux at the center of the anode and cathode

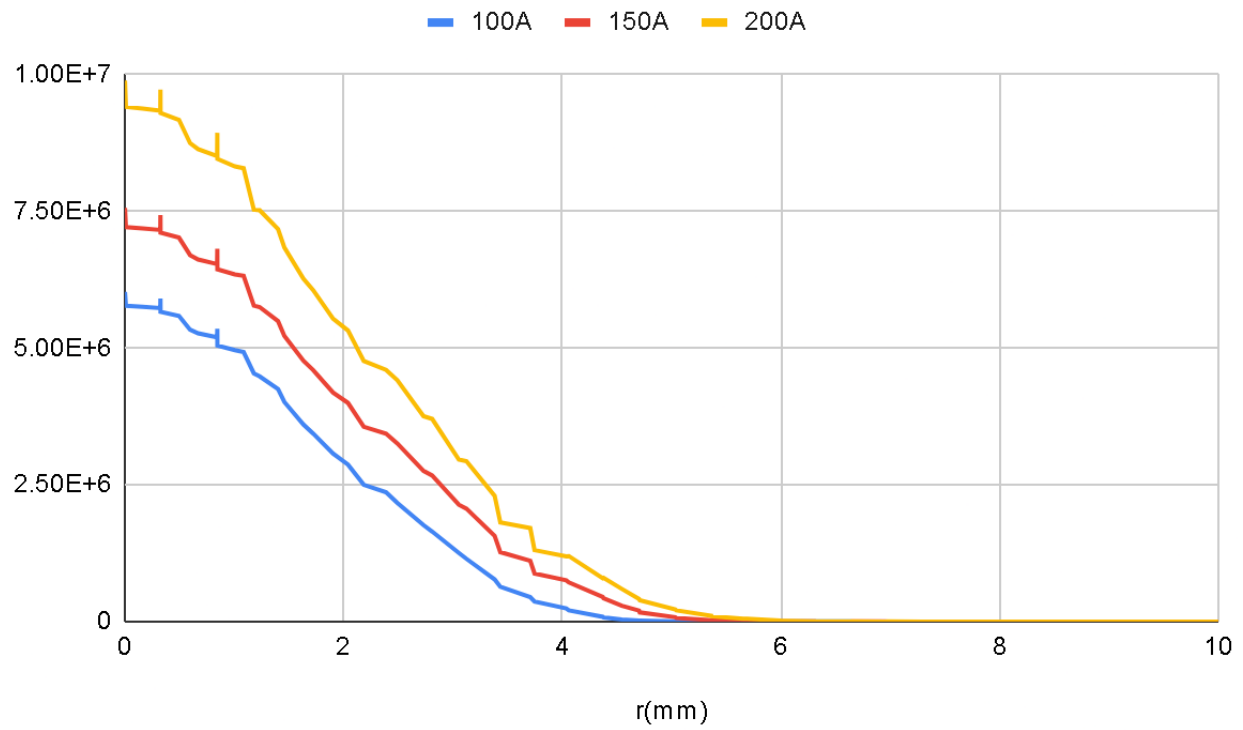


Figure 20: Radial evolution of Current Density at the center of the anode and cathode

<b>Input Current</b>	100A	150A	200A
<b>Max Temperature</b>	13019 K	13637 K	14458 K
<b>Max Pressure</b>	77 Pa	149 Pa	274 Pa
<b>Max HeatFlux</b>	13428311 W/m <sup>2</sup>	20561396 W/m <sup>2</sup>	3.97E+07 W/m <sup>2</sup>
<b>Max Current Density</b>	15659279 A/m <sup>2</sup>	20526947 A/m <sup>2</sup>	27763394 A/m <sup>2</sup>

**Table 9: Parameters at 60 degrees**

### 2.3.3 90° Electrode Sharpening Angle

Figs 21, 22 and 23 show the temperature profile for different input currents 100A, 150A, 200A respectively for the electrode sharpening angle of 90°. From these figures, it is again observed that increasing the input current widens the concentration zone of temperature at the anode.

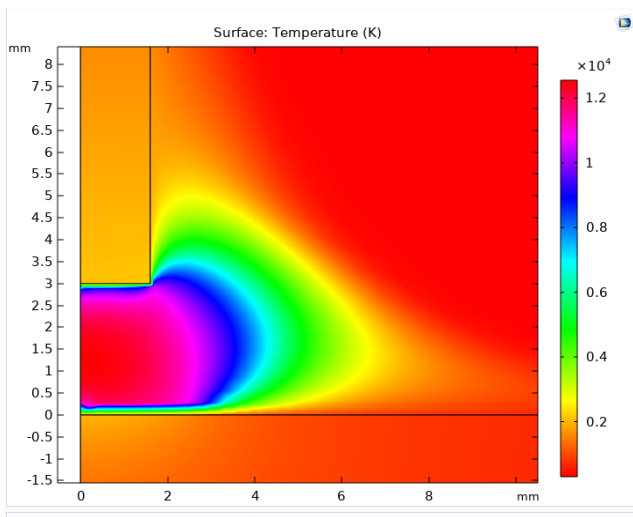


**Fig 21: Temperature Profile at 100A**

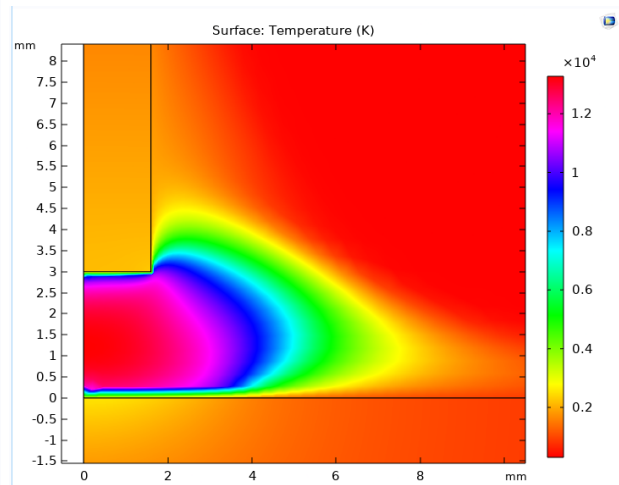


**Fig 22: Temperature Profile at 150A**

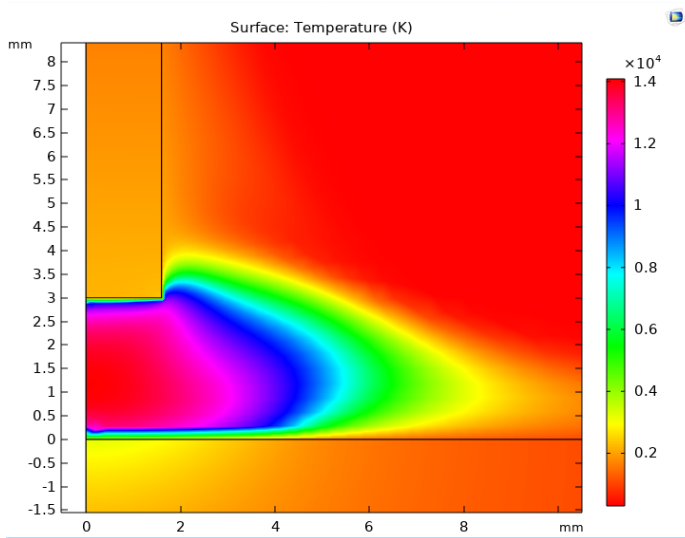


**Fig 23: Temperature Profile at 200A**

The radial evolution of temperature, pressure, heat flux, and current density at the center of the cathode and anode for the different input currents are shown in Fig 24,25,26, and 27 respectively. From the figure, it can be seen that all of these properties are typically following gaussian distribution.

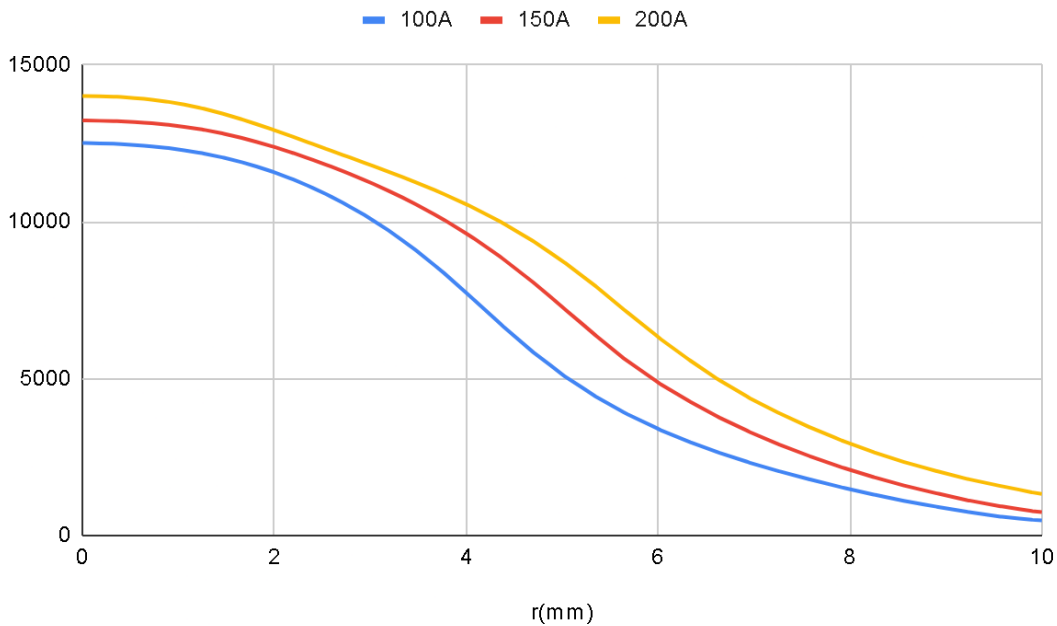


**Figure 24: Radial evolution of Temperature at the center of the anode and cathode**

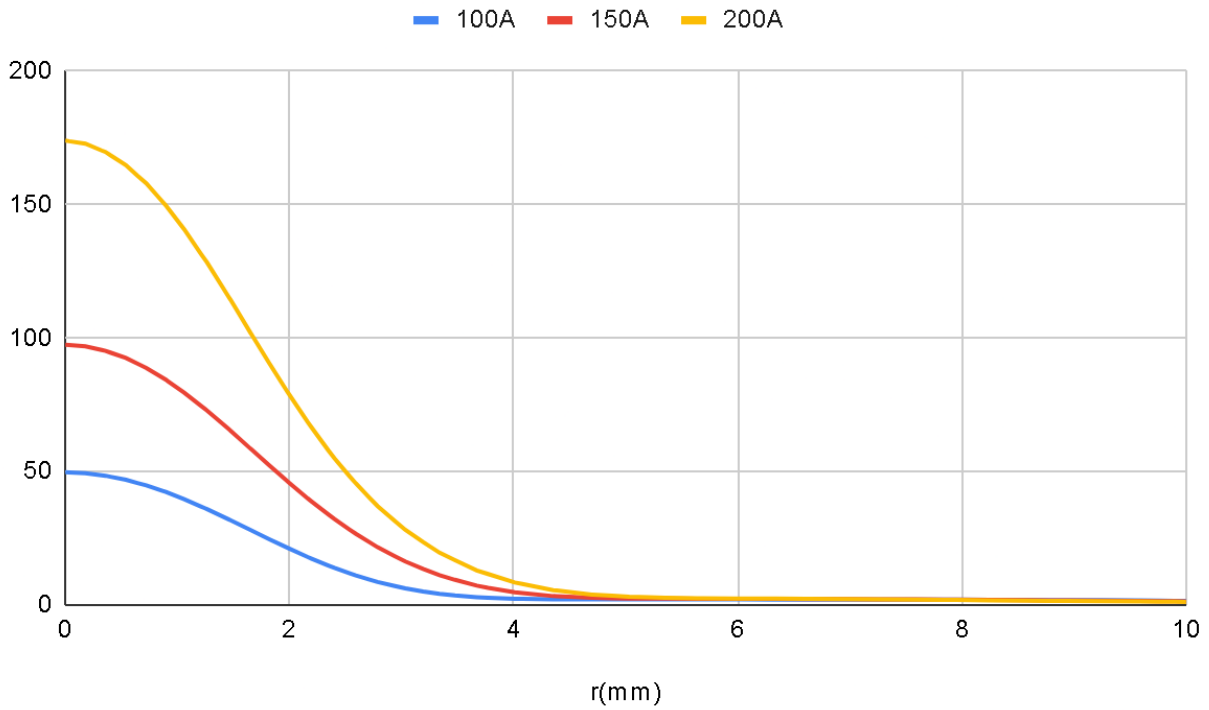


**Figure 25: Radial evolution of Pressure at the center of the anode and cathode**

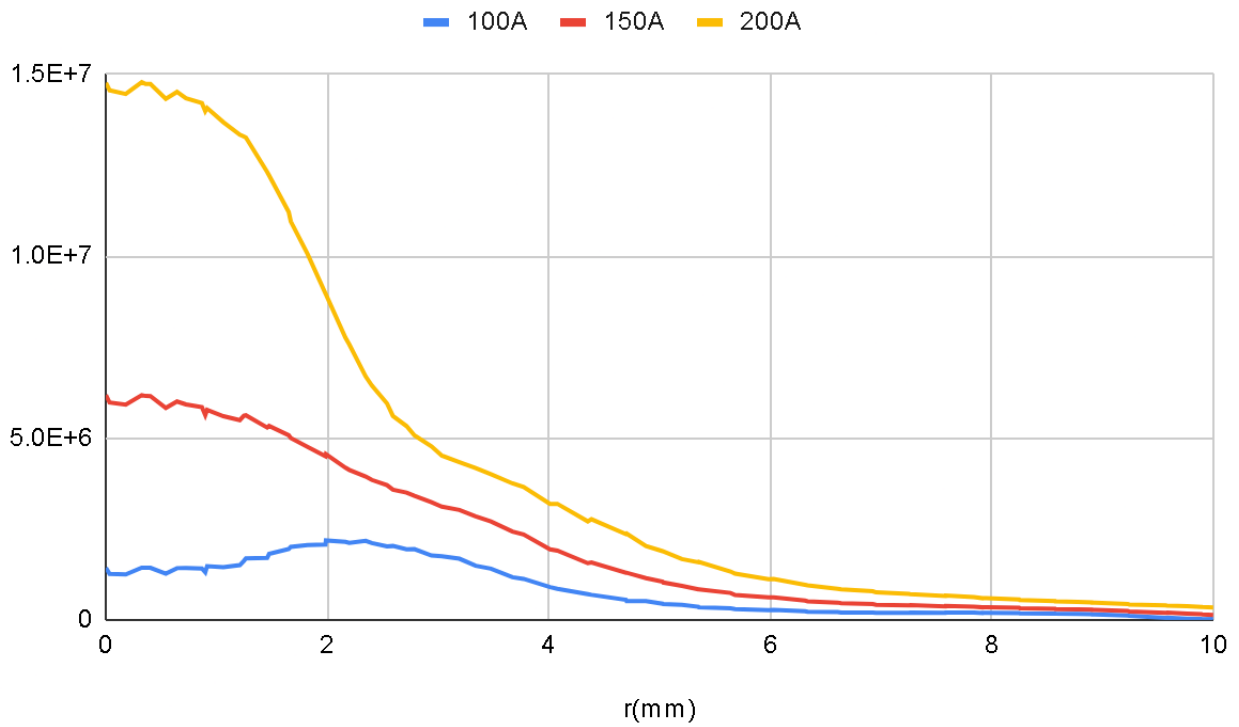


**Figure 26: Radial evolution of HeatFlux at the center of the anode and cathode**

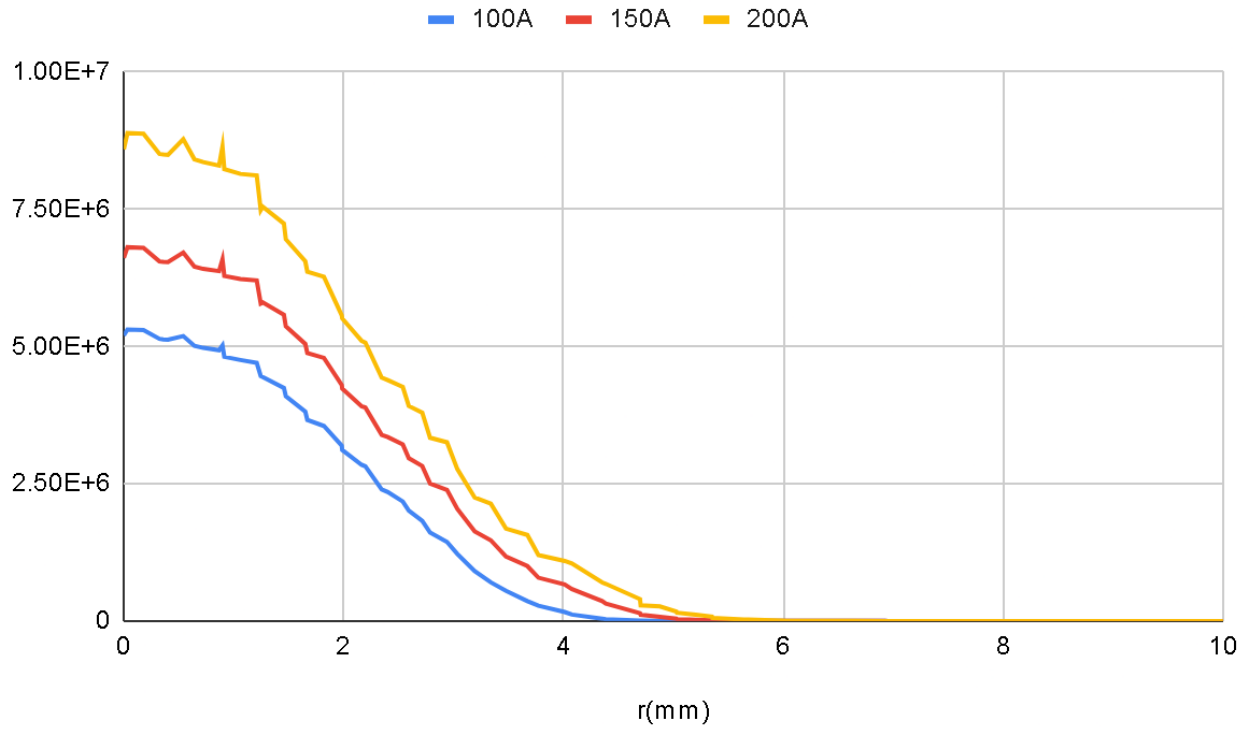


Figure 27: Radial evolution of Current Density at the center of the anode and cathode

Input Current	100A	150A	200A
Max Temperature	12552 K	13273 K	14087 K
Max Pressure	53 Pa	105 Pa	192 Pa
Max HeatFlux	5918005 W/m <sup>2</sup>	7916295 W/m <sup>2</sup>	15277662 W/m <sup>2</sup>
Max Current Density	7123980 A/m <sup>2</sup>	9916961 A/m <sup>2</sup>	1.36E+07 A/m <sup>2</sup>

Table 10: Parameters at 90 degrees

### 2.3.4 107° Electrode Sharpening Angle

Figs 28, 29 and 30 show the temperature profile for different input currents 100A, 150A, 200A respectively for the electrode sharpening angle of 107°. From these figures, it is again observed that increasing the input current widens the concentration zone of temperature at the anode.

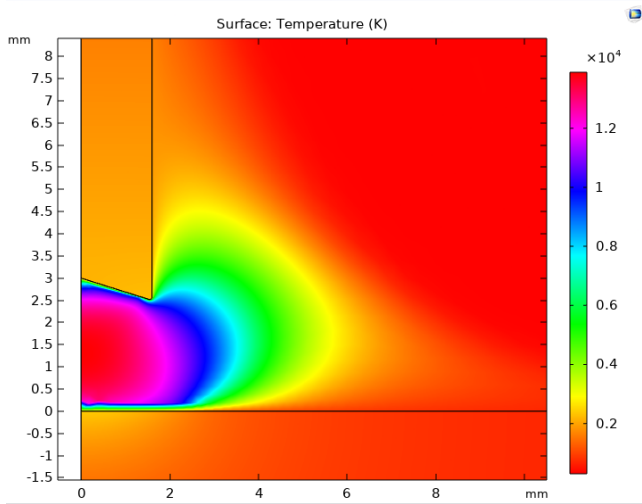


Fig 28: Temperature Profile at 100A

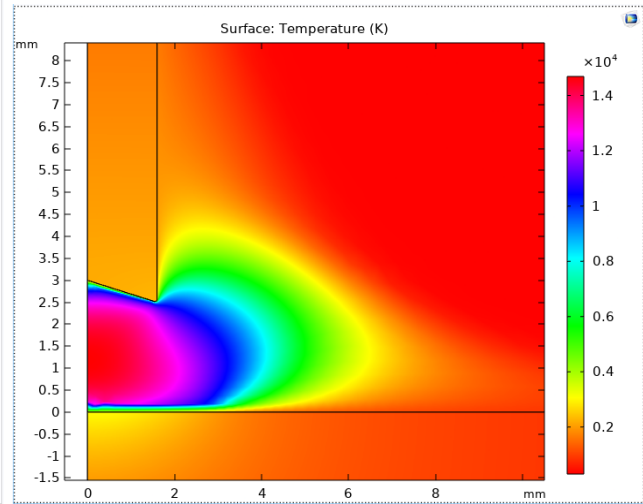


Fig 29: Temperature Profile at 150A

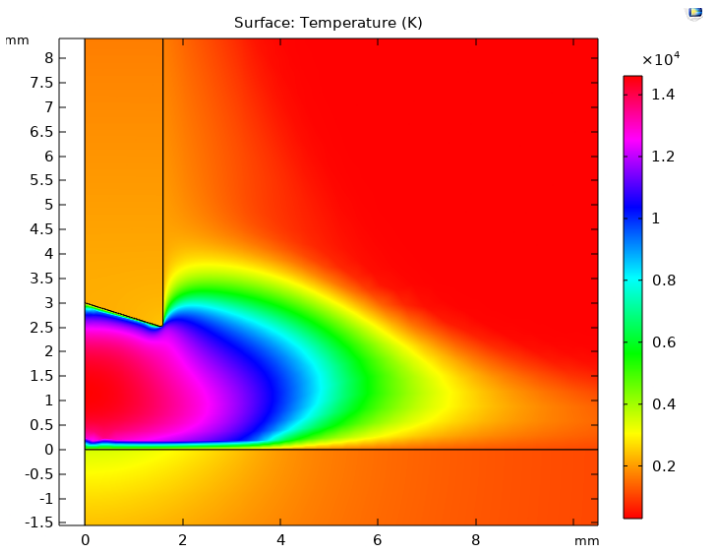
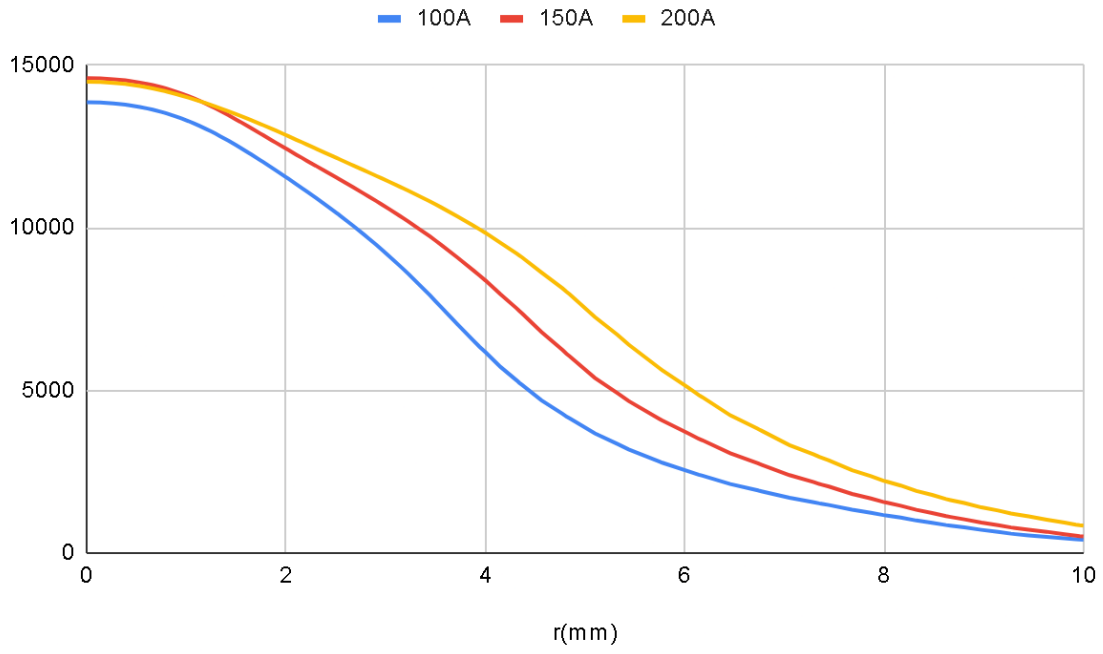
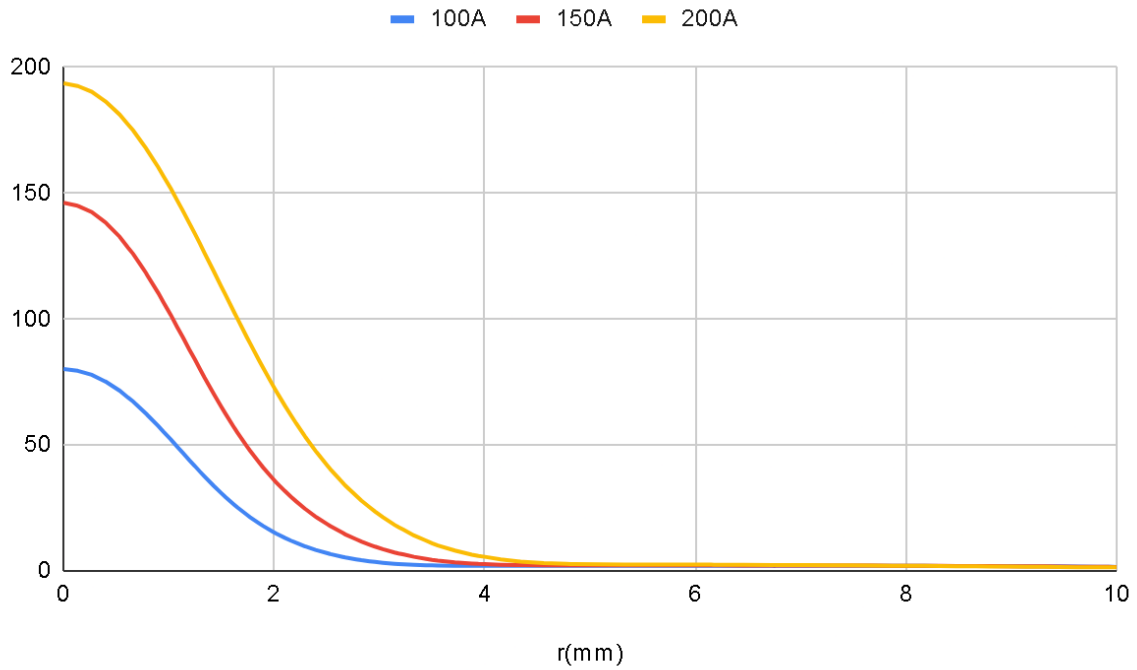


Fig 30: Temperature Profile at 200A



**Figure 31: Radial evolution of Temperature at the center of the anode and cathode**



**Figure 32: Radial evolution of Pressure at the center of the anode and cathode**

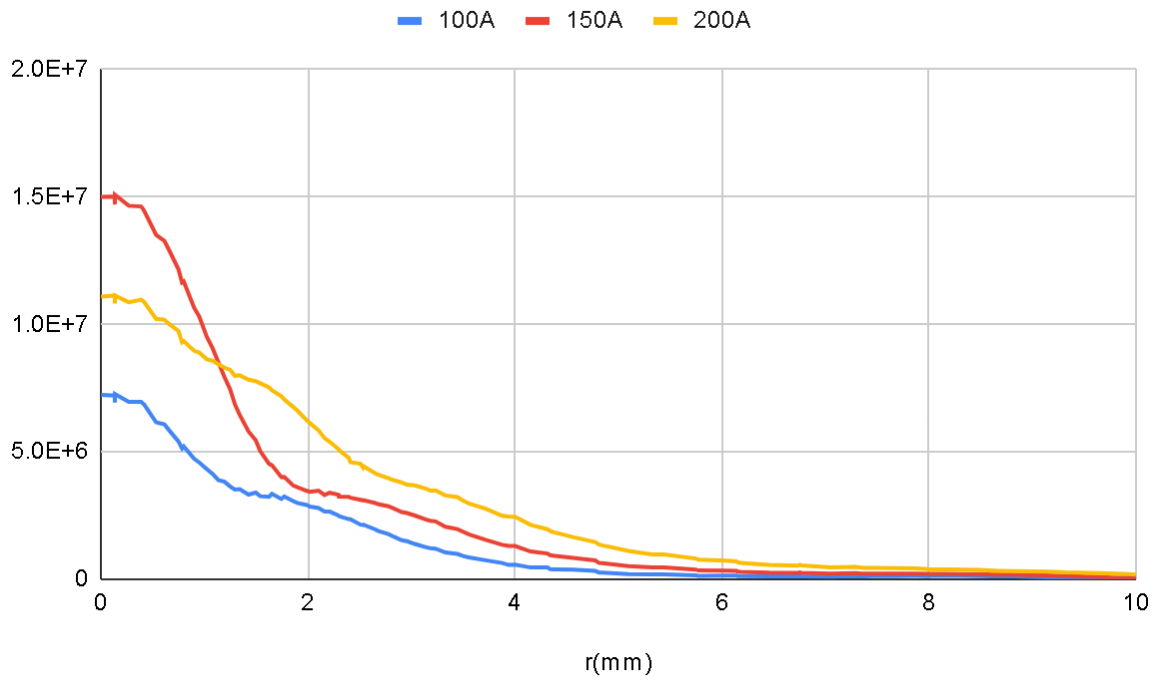


Figure 33: Radial evolution of HeatFlux at the center of the anode and cathode

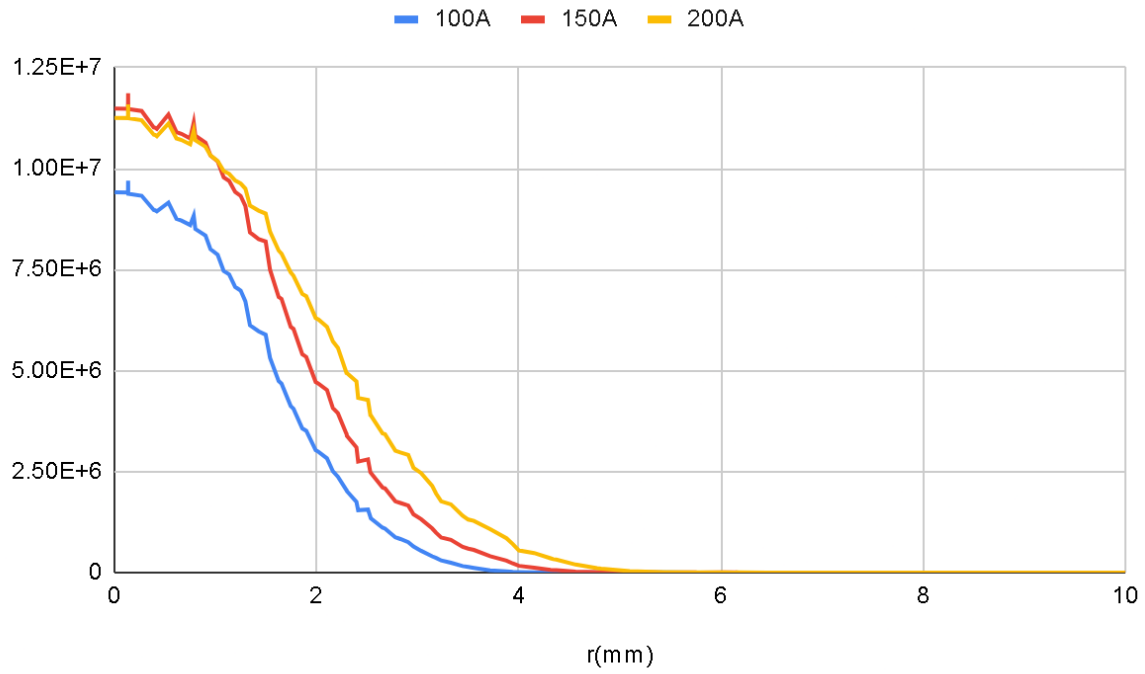


Figure 34: Radial evolution of Current Density at the center of anode and cathode

The radial evolution of temperature, pressure, heat flux, and current density at the center of cathode and anode for the different input currents are shown in Fig x,y,z, and w respectively. From the figure, it can be seen that all of these properties are typically following gaussian distribution.

<b>Input Current</b>	100A	150A	200A
<b>Max Temperature</b>	13894 K	14688 K	14609 K
<b>Max Pressure</b>	90 Pa	162 Pa	204 Pa
<b>Max HeatFlux</b>	12700721 W/m <sup>2</sup>	17158570 W/m <sup>2</sup>	14461822 W/m <sup>2</sup>
<b>Max Current Density</b>	11523853 A/m <sup>2</sup>	13798444 A/m <sup>2</sup>	1.32E+07 A/m <sup>2</sup>

**Table 11: Parameters at 107degree**

## 2.4 Experiment:

The setup used in the experiment is developed in-house, with 4-axis CNC. It was driven by hybrid servo motors(3-70 kg-cm torque) with RHINO motion controls drivers.

### 2.4.1 Experimental Setup

The setup shown in fig. x has one CNC setup consisting of 3 linear axes and an electrode attached to a TIG torch, one load controller. These axes of CNC are controlled by mach3 CNC software.

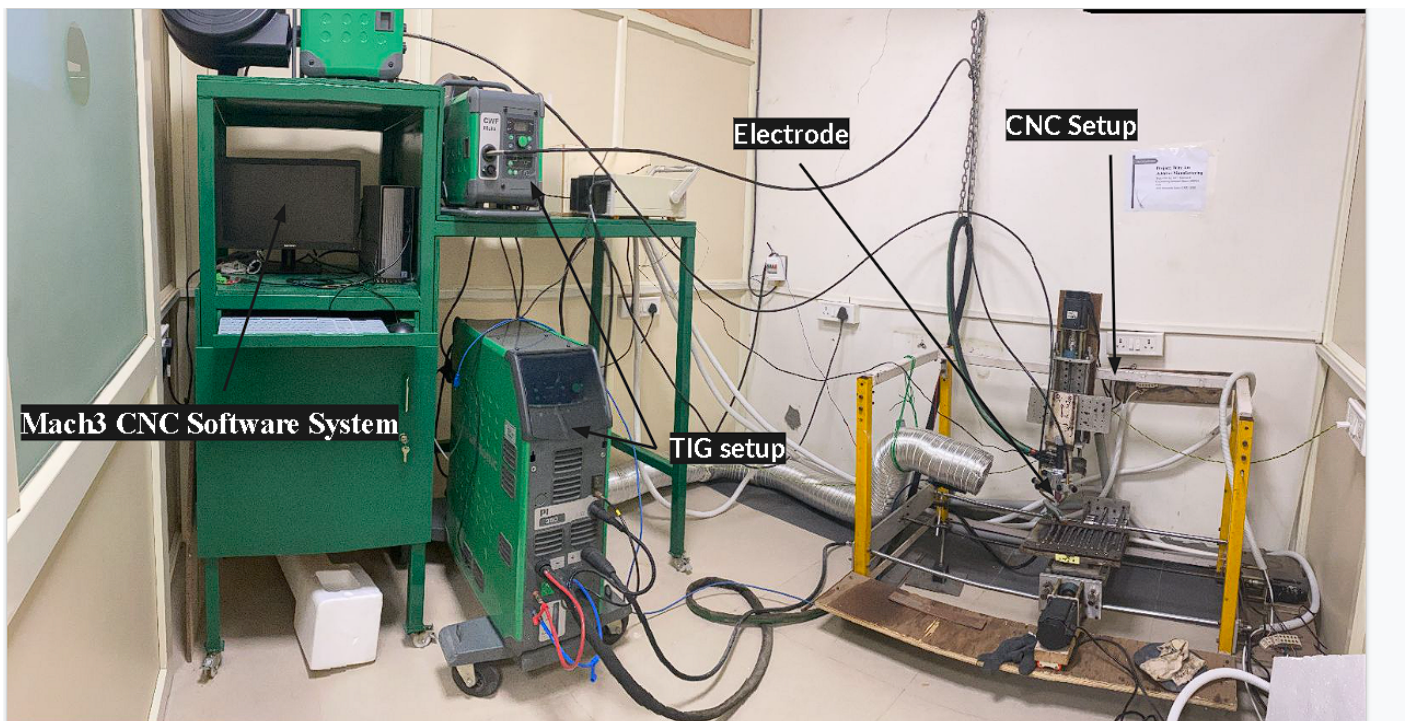


Figure 35: Experimental setup

### 2.4.2 Mach3 CNC Software

Mach3 CNC software is used to control the CNC setup. RNR Universal USB Motion Circuit board is designed for Mach3 software. This Circuit Board supports up to 4-axes control. The programming in software was done in standard ‘G’ and ‘M’ coding. The USB interface of the circuit board is suitable for any laptop, desktop, or tablet PC.

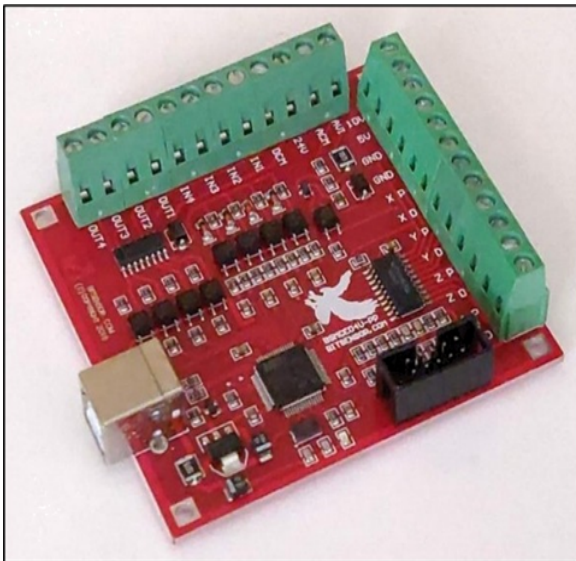


Figure 36. ' Mach3 Control Board

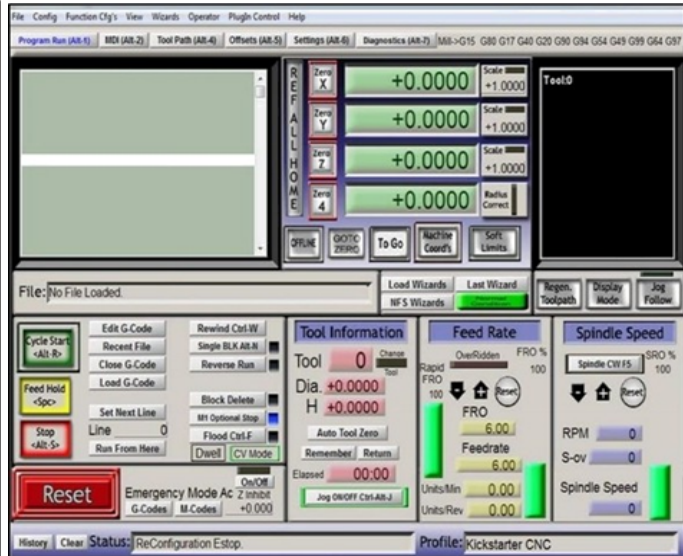


Figure 37. ' Mach3 Control Software

### 2.4.3 Observations

Below Figures show the TIG arc profile for different input currents 100A, 150A, and 200A at different sharpening angles of 90,67, and 50 degrees respectively

1.) at 90° sharpening angle

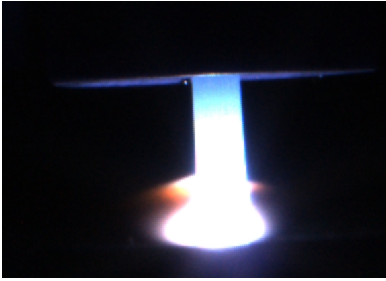


figure 38: 100A

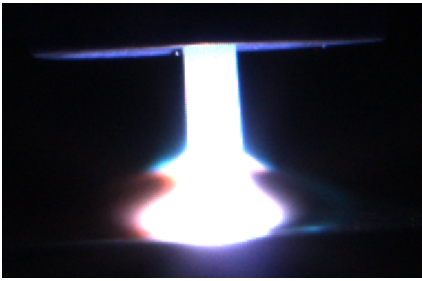


figure 39: 150A

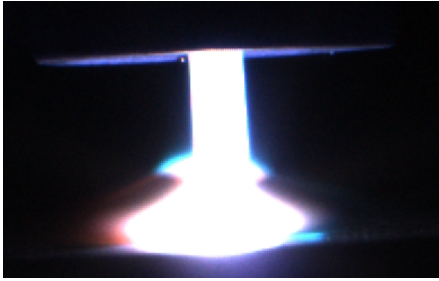


figure 40: 200A

2.) at 67° sharpening angle



figure 41: 100A

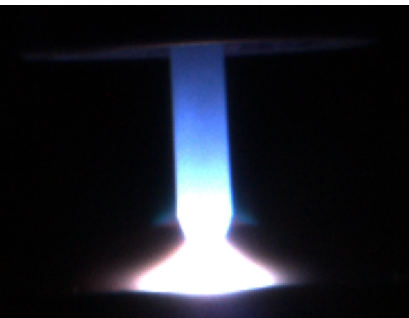


figure 42: 150A

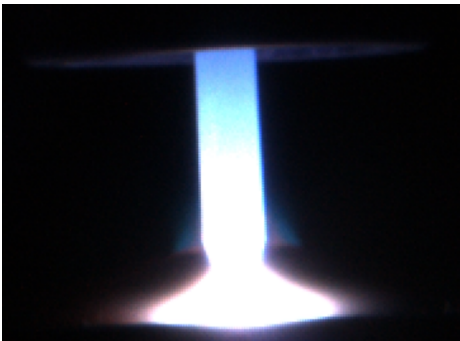


figure 43: 200A

3.) at 50° sharpening angle

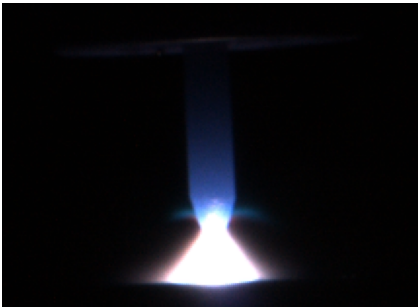


figure 44: 100A

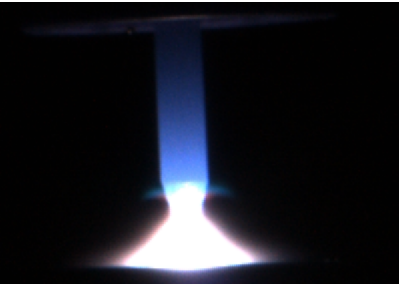


figure 45: 150A

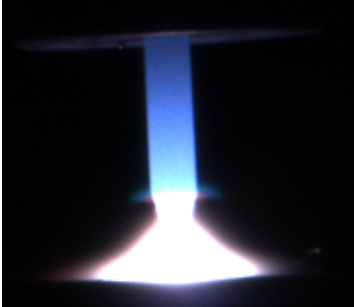


figure 46: 200A



## Chapter3: Results and Discussion

We have done simulation and experimentation for the different electrode sharpening angles at different current inputs 100A, 150A, and 200A. Figure 45 and 46 show the temperature profile (simulation) at a 60-degree sharpening angle and experimental arc at a 67-degree sharpening angle with 100A, 150A, and 200A current input respectively.

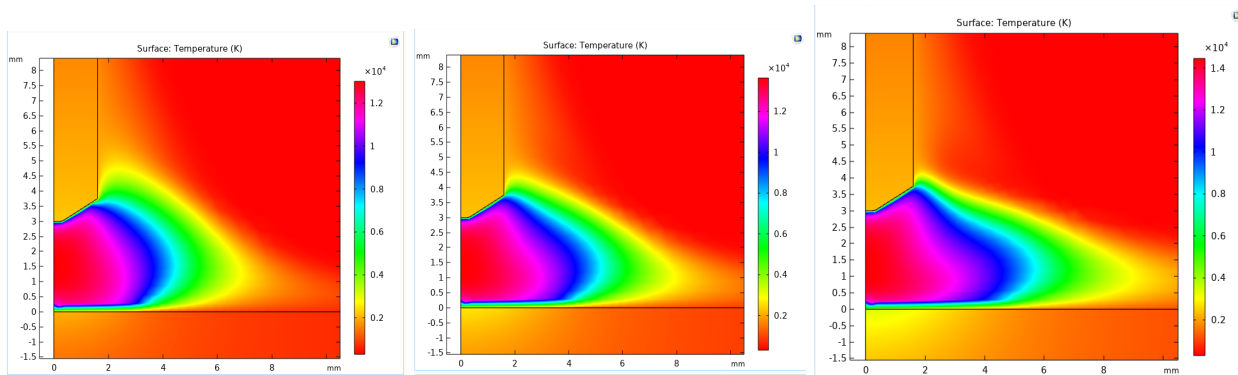


Figure 47: temperature profile at 100A, 150A, and 200A respectively at 60-degree sharpening angle

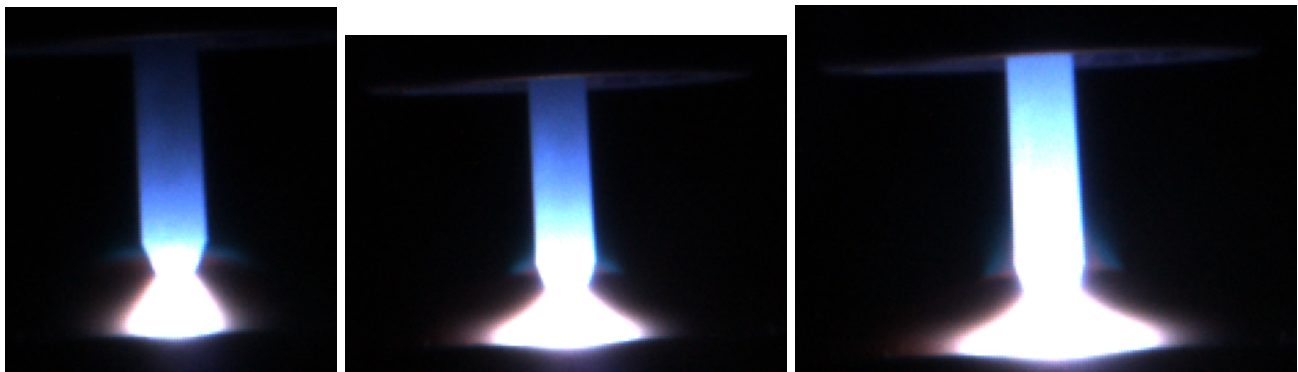


Figure 48: temperature profile at 100A, 150A, and 200A respectively at 67-degree sharpening angle

From the arc temperature profiles (simulation ), It is observed that the increase in input current widens the concentration zone at the anode. Experiment results also confirm the same

The Figures shown in section 2.3 show the radial evolution of temperature, Pressure, Heat Flux, and current density at the center of the cathode and anode for different electrode sharpening angles of 30, 60, 90, and 107 different input currents values 100A, 150A, and 200A. From there It is observed that temperature, pressure, heat flux, and current density all of these are typically following Gaussian distribution

Figures x show the heat flux variation across arc length at different electrode sharpening angles and 150A input current

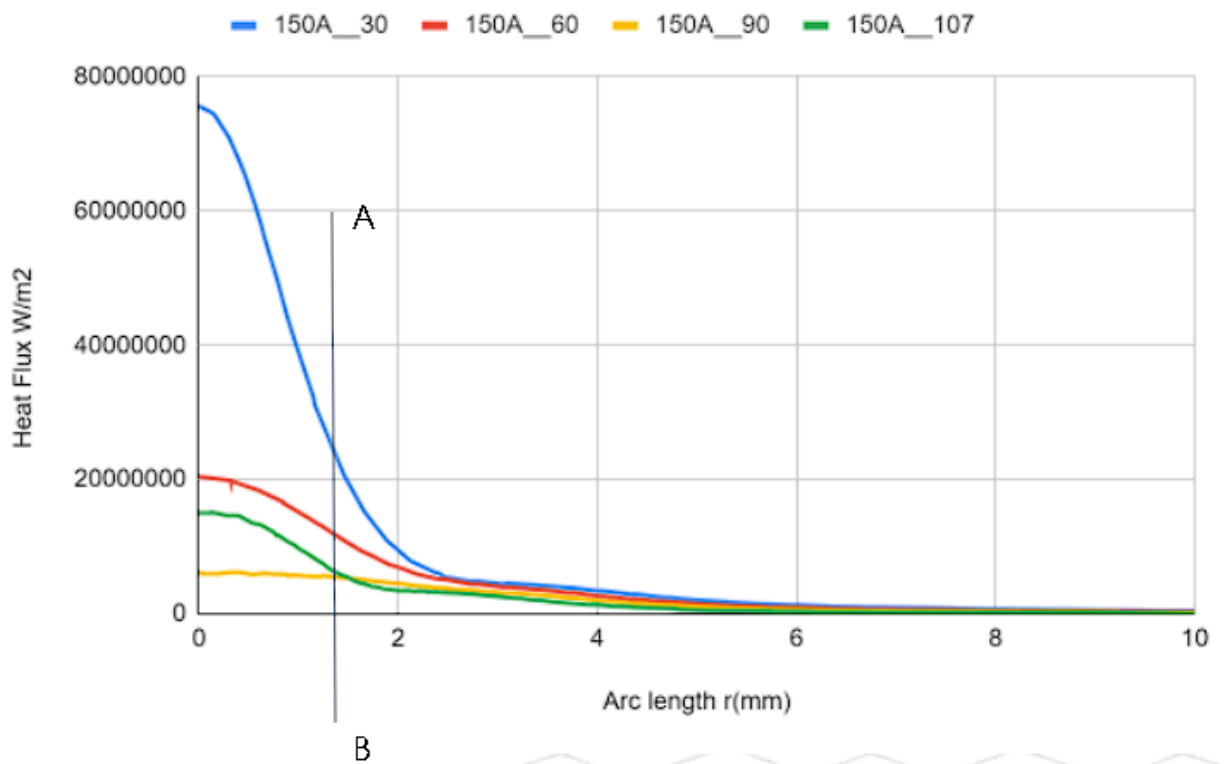


Figure 49: the heat flux variation across arc length at different electrode sharpening angles and 150A input current

$$\% \text{ Area} = \frac{\text{Area Under graph till line AB}}{\text{Total Area under graph}}$$

More the % Area for any graph more will be the concentration of graphs in a narrower area. From figure x, it can be seen that the % area is more in the case of 30 degrees in comparison to 60 and 90-degree sharpening angles. As we are increasing the sharpening angle, % the area is decreasing which means less concentration in narrow areas.

For the Better process efficiency in WAAM application, we required a more uniform distribution compared to intense distribution which is achieved at a higher sharpening angle according to our results from simulations and experiments.



## **Chapter4: Conclusion and Future Scope**

### **4.1 Conclusion**

Simulations and Experimental investigation of the effect of electrode shape and Input current load on the Tig arc behavior are presented in this work. These parameters have significant impacts on arc properties:

1. The increase in arc input current widens the concentration zone at the anode.
2. Temperature, Heat Flux, pressure, and current density all of these properties typically follow the Gaussian distribution.
3. An increase in electrode sharpen angle increases the arc concentration to a narrow area and vice versa

### **4.2 Future Scope:**

The scope of the work that can be done in the future to improve the WAAM process efficiency using the shape of electrode:

- a. Experiment could be conducted with more variation in sharpening angle with wire feeding.
- b. An increase in electrode sharpening angle increases the uniform distribution of energy, This need to be tested from the experiment.
- c. In the present work, only the electrode tip shape was changed and the electrode itself was in a cylindrical shape. The simulation could be done for more electrode shapes like rectangular, triangular, etc.



## References

- 1.) Abderrazak Traidia, Frederic Roger, A. Chidley: Effect of helium-argon mixtures on the heat transfer and fluid flow in Gas Tungsten Arc Welding  
[https://www.researchgate.net/publication/298450385\\_Effect\\_of\\_helium-argon\\_mixtures\\_on\\_the\\_heat\\_transfer\\_and\\_fluid\\_flow\\_in\\_Gas\\_Tungsten\\_Arc\\_Welding](https://www.researchgate.net/publication/298450385_Effect_of_helium-argon_mixtures_on_the_heat_transfer_and_fluid_flow_in_Gas_Tungsten_Arc_Welding)
- 2.) X. Yang, Y. Song, K. Hu, Y. Xia: Characteristic of energy distribution at anode and cathode on AC TIG welding arc  
[https://www.researchgate.net/publication/282820775\\_Characteristic\\_of\\_energy\\_distribution\\_at\\_anode\\_and\\_cathode\\_on\\_AC\\_TIG\\_welding\\_arc](https://www.researchgate.net/publication/282820775_Characteristic_of_energy_distribution_at_anode_and_cathode_on_AC_TIG_welding_arc)
- 3.) C.S.Wu, M.Ushio, M.Tanaka: Analysis of the TIG welding arc behavior  
<https://www.sciencedirect.com/science/article/pii/S0927025696000481>
- 4.) COMSOL Module: Plasma DC Arc  
<https://www.comsol.com/model/plasma-dc-arc-97661#comsol60>
- 5.) COMSOL Documentation  
<https://doc.comsol.com/6.0/docserver/#!/com.comsol.help.comsol/helpdesk/helpdesk.html>

